Published in IET Power Electronics
Received on 13th May 2009
Revised on 6th November 2009
doi: 10.1049/iet-pel.2009.0132

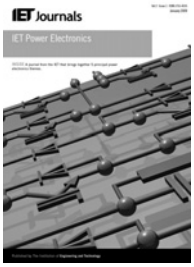

ISSN 1755-4535

Grid synchronisation with harmonics and reactive power compensation capability of a permanent magnet synchronous generator-based variable speed wind energy conversion system

M. Singh[1] *V. Khadkikar*[2] *A. Chandra*[1]

[1]*Department of Electrical Engineering, Ecole de technologie superieure, 1100, Rue Notre-Dam Ouest, Montreal, Quebec, Canada H3C 1K3*
[2]*Electrical and Computer Engineering Department, The University of Western Ontario, London, Ontario, Canada N6A 5B9*
E-mail: smukhtiar_79@yahoo.co.in

Abstract: The power electronics plays an important role in the reliable operation of a modern wind energy conversion system (WECS). This study aims at the grid interconnection of a permanent magnet synchronous generator (PMSG)-based wind turbine with harmonics and reactive power compensation capability at the point of common coupling (PCC). The proposed system consists of two back-to-back connected converters with a common dc-link. The generator-side converter is used to achieve maximum power point tracking (MPPT). The grid-side converter is actively controlled to feed generated power as well as to supply the harmonics and reactive power demanded by the non-linear load at PCC, thus enabling the grid to supply only sinusoidal current at unity power factor. A model of directly driven PMSG-based variable speed WECS is developed and simulated in MATLAB/SPS environment. The effectiveness of proposed control approach is validated through extensive simulation and experimental results.

1 Introduction

The alternative energy resources have recently attracted lot of interest because of increasing pollution level and depleting fossil fuels. Among renewable energy sources, wind energy generation has been noted as the most rapidly growing technology, being one of the most cost-effective and environmental friendly means to generate electricity from renewable sources. Thanks to recent development in wind power technology, the modern wind turbines are now being deployed world wide in large scale. The advancement in power electronics devices has further played an important role in the improvement of their reliability and controllability.

In the early 1980s, the wind farms were installed with the help of financial support and incentives from government. The low penetration level of wind turbine during these early periods may have very little impact on the operational behaviour, reliability and security of grid. However, in the present scenario, the increasing penetration level of wind turbines has made it mandatory to take them in account while determining the stability of the grid [1–3]. The modern wind turbines are not only required to supply power but also support the grid during any kind of fault and voltage unbalance. This kind of ability of wind turbines is known as ride-through capability. The wind energy conversion system (WECS) should also be able to control its output reactive power automatically as a function of voltage at PCC. The conventional WECS usually consists of static VAR compensators, static-compensators or synchronous compensators for voltage stability at the point of common

doi: 10.1049/iet-pel.2009.0132

coupling (PCC) [4]. Modern wind turbines have several commercially available topologies mainly based on induction generator, doubly fed induction generator and synchronous generator with innovative power electronics interface [5, 6]. Owing to intensified grid codes, the wind turbines with full-scale converters will be preferred in future, as the power converters fully decouples the wind turbine from grid disturbances and can be helpful in some sort of grid support. The major drawback of full converter rating is their higher installation cost. Moreover, because of the intermittent nature of wind, the full converter rating is rarely utilised. Besides this, the increasing penetration level of WECS may lead to grid instability or even failure, if these systems are not controlled properly.

This paper proposes a novel control strategy for grid interconnection of WECS and to solve the power quality problem at PCC. The system under consideration employs PMSG-based variable speed WECS consisting of two back-to-back converters with a common dc-link. The generator-side converter controls generator speed in order to achieve maximum power point tracking (MPPT). The grid-side inverter regulates dc-link voltage and injects the generated power into the grid. In addition to this, the grid-side inverter is also utilised to compensate the reactive power and current harmonics generated by non-linear loads, if any, at PCC. This enables the grid to supply only sinusoidal current at unity power factor (UPF). The proposed control strategy utilises the grid-side inverter rating optimally which is always underutilised because of lower wind capacity factor. According to the authors of [7–9], the expected wind output during peak is nearly 60% of rated output, and yet the annual capacity factor may be in the 20–30% range. Thus, the proposed strategy helps to achieve IEEE standard requirements with improved power quality at PCC. The simulation and experimental results are provided to validate the active power injection as well as the harmonics and reactive power compensation capabilities simultaneously.

The paper is organised as follows: the system under consideration is discussed in Section 2. The proposed control strategy for generator- and grid-side converters is explained in Section 3. The MATLAB/SPS-based simulation results are given in Section 4 and the experimental results are discussed in Section 5. Section 6 concludes the paper.

2 System description

The system under consideration employs PMSG-based variable speed WECS consisting of two back-to-back converters with a common dc-link. The block diagram of variable speed WECS is shown in Fig. 1 and the main components of system with their important characteristics are discussed below.

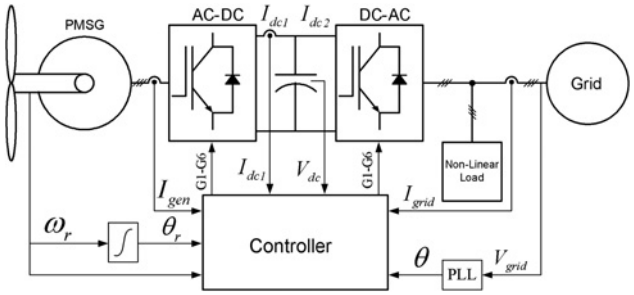

Figure 1 *Block diagram of PMSG-based variable speed WECS*

2.1 Wind turbine

The wind power captured by wind turbine depends on its power co-efficient (C_p) which is given by the relation

$$C_p = \frac{P_{\text{turb}}}{P_{\text{wind}}} \tag{1}$$

$$P_{\text{turb}} = P_{\text{wind}}\, C_p = \frac{1}{2}\,\rho\,\pi\, r^2\, V_\omega^3\, C_p \tag{2}$$

where ρ is the air density, V_ω is the wind velocity and r is the radius of circular swept area of rotor blades.

But, for a given turbine C_p is not always constant. The most common parameters for C_p are the tip speed ratio λ and the pitch angle β. The tip speed ratio is given as

$$\lambda = \frac{\text{tip speed}}{\text{wind speed}} = \frac{\omega_r \cdot r}{V_\omega} \tag{3}$$

Here the power coefficient $C_p = f(\lambda, \beta)$ is a function of both parameters. Consequently, different wind speeds will require the optimal values of tip speed and pitch angle to achieve a high C_p and therefore giving the highest power output at all available wind speeds [10–12]. The above-mentioned aspects make it very clear that to extract maximum power out of the varying wind we need to have a wind turbine that allows the change in rotor speed to reach optimal aerodynamic conditions. As every optimal $C_{p,\text{optimal}}$ has one optimal value of tip speed ratio λ_{optimal}, it is necessary to control the tip speed ratio according to the wind speed. This task of MPPT is achieved by using power co-efficient against tip speed ratio for different pitch angles of the turbine. The active pitch control is used during high wind velocity to shed off the aerodynamic power by turning the rotor blades through some angle from the direction of striking wind (also known as pitch angle control). The aerodynamic power captured by wind turbine is the cosine function of pitch angle. In this paper, the pitch angle is kept zero, which is a valid assumption for lower to medium wind velocities.

2.2 Generator

Recently the PMSG has been gaining a lot of attention for WECS because of compact size, higher power density, reduced losses, high reliability and robustness. Moreover, there is a need of low-speed gearless generator, especially for off-shore wind applications, where the geared doubly fed induction generator or induction generator will require regular maintenance because of tearing–wearing in brushes and gear box. Both the brushes and the gear box can be eliminated from WECS by using directly coupled low-speed generators. Further, the elimination of the gear box can increase the efficiency of wind turbine by 10% [13].

The low-speed PMSG requires:

1. higher number of poles to obtain suitable frequency at low speed;

2. big rotor diameter for the high wind turbine torque.

The dynamic model of PMSG can be represented in a rotating reference frame with the help of following equations [13, 14]

$$V_q = R_s i_q + L_q \frac{\mathrm{d}i_q}{\mathrm{d}t} + \omega_r L_d i_d + \omega_r \lambda_m \tag{4}$$

$$V_d = R_s i_d + L_d \frac{\mathrm{d}i_d}{\mathrm{d}t} - \omega_r L_q i_q \tag{5}$$

The expression for electromagnetic torque in the rotor can be written as

$$T_e = \left(\frac{3}{2}\right)\left(\frac{P}{2}\right)[(L_d - L_q) i_q i_d - \lambda_m i_q] \tag{6}$$

In case of a cylindrical rotor, L_d; L_q and hence the above equation reduces to

$$T_e = \left(\frac{3}{2}\right)\left(\frac{P}{2}\right)\lambda_m i_q \tag{7}$$

where P is the number of poles, λ_m is magnetic flux, L_d is direct-axis inductance, L_q is quadrature inductance, R_s is resistance and ω_r is rotor speed of the generator.

2.3 Power electronics interface

Several types of power electronic interfaces have been investigated for variable speed wind turbines [15–17]. The proposed system consists of two back-to-back fully controlled converters decoupled by a dc-link. The converters have been realised by using six switches for each converter. Since PMSG is connected to the grid through an ac/dc/ac system, the power generated (P_{Gen}) by PMSG is first transferred to dc-link and then from dc-link to grid. The exchange of reactive power cannot take place because of the presence of dc-link. The generator-side converter injects current I_{dc1} into dc-link at voltage level V_{dc}

$$I_{dc1} = \frac{P_{Gen}}{V_{dc}} \tag{8}$$

whereas the current received on the other side of dc-link is

$$I_{dc2} = \frac{P_{dc}}{V_{dc}} = \frac{P_S + P_{Loss}}{V_{dc}} \tag{9}$$

where P_{dc} is the power at dc-link, P_S is active power supplied to the grid and P_{Loss} denotes converter losses. If converter losses are negligible then $P_{Gen} = P_{dc} = P_S$.

3 Development of the proposed control strategy

In this section the proposed control strategy for generator- and grid-side converters is discussed.

3.1 Generator-side converter control

In a variable speed WECS, the maximum power at different wind velocities is almost a cubic function of generator speed as shown in Fig. 2. Therefore the generator speed is controlled in order to follow the power-speed characteristic. For this purpose, the power at dc-link is used to obtain reference speed by using the power-speed curve of the generator. The error of this reference speed and actual speed is then given to the proportional-integral (PI) regulator to obtain reference torque of the generator expressed as

$$T_e^* = \left(K_{P\omega} + \frac{K_{I\omega}}{S}\right)(\omega_r^* - \omega_r) \tag{10}$$

where $K_{P\omega}$, $K_{I\omega}$ are proportional and integral gains for generator speed control.

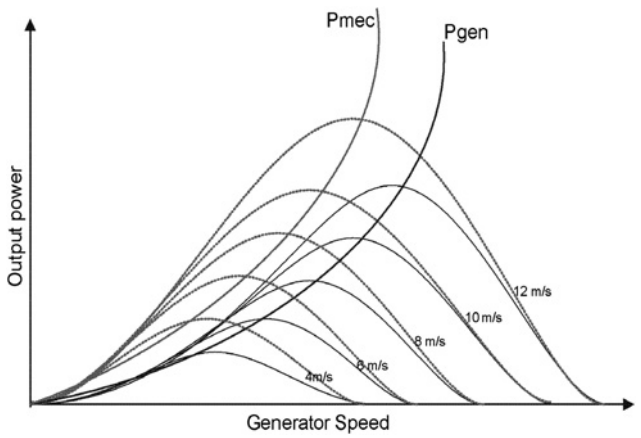

Figure 2 *Generator power-speed characteristics at various wind velocities*

Here P_{mec} is the power captured by wind turbine and P_{gen} is generator output power

doi: 10.1049/iet-pel.2009.0132

The q-axis reference current component (torque controlling current component) can be derived using (7)

$$i_q^* = \frac{4}{3}\left(\frac{T_e^*}{P\lambda_m}\right) \tag{11}$$

The d-axis reference current component can be set to zero in order to obtain maximum torque at minimum current and therefore to minimise the resistive losses in the generator [18]. The generator-side control diagram is shown in Fig. 3.

3.2 Grid-side converter control

The grid-side inverter is used to regulate dc-link voltage so that the power balance can be maintained under both fluctuating wind and grid disturbances. The control of this grid-side inverter comprises two cascaded loops. The outer dc-voltage control loop is used to set the current reference for active power control. The inner current loop is used to achieve harmonic and reactive power compensation, as per the demand of non-linear load at PCC. The proposed control strategy is realised in a synchronous rotating reference frame. By means of this reference frame, the control variables become dc quantities; thus, filtering and controlling can be easily achieved. Moreover, the PI regulator gives an enhanced performance while regulating dc variables [19].

The basic principle of the proposed control strategy is derived from a three-phase shunt active power filter, where the inverter current consists of two components: harmonic compensation current, i_h and active current component in proportional to generated wind power i_w. Thus, the current

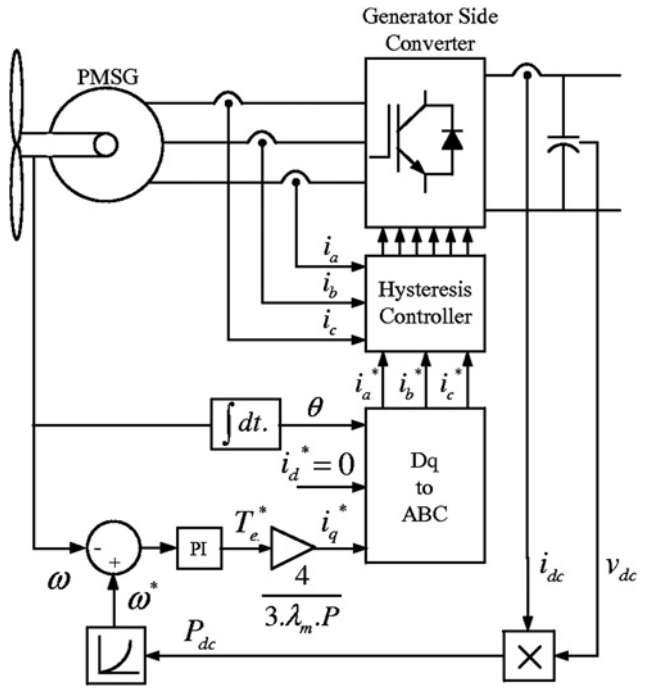

Figure 3 *Generator-side converter control*

injected from the inverter into the grid can be given as

$$i_{inv} = i_h + i_w = i_g - i_L \tag{12}$$

where i_g is the grid current and i_L is the non-linear load current to be compensated at the PCC. The non-linear load may consist of three components, the fundamental active component (in-phase component), the reactive component (quadrature component) and the harmonic currents (or harmonic reactive component). Therefore if the grid-side inverter supplies the active current proportional to generated wind power, the reactive and harmonic currents of non-linear load, then the grid needs only to supply active current to the load at PCC.

Let the three-phase grid-side voltages be as follows

$$\left.\begin{aligned} e_a &= E\cos(\omega t) \\ e_b &= E\cos\left(\omega t - \frac{2\pi}{3}\right) \\ e_c &= E\cos\left(\omega t + \frac{2\pi}{3}\right) \end{aligned}\right\} \tag{13}$$

where E is the maximum phase voltage and ω is the angular frequency of the grid-side supply. From (12), the load currents i_{La}, i_{Lb} and i_{Lc} are the algebraic sum of injected inverter currents and the grid currents of each phase as follows

$$\left.\begin{aligned} i_{La} &= i_{ga} - i_{inva} \\ i_{Lb} &= i_{gb} - i_{invb} \\ i_{Lc} &= i_{gc} - i_{invc} \end{aligned}\right\} \tag{14}$$

where i_{ga}, i_{gb}, i_{gc} are grid currents and i_{inva}, i_{invb}, i_{invc} are inverter injected currents.

The voltage equations in a-b-c frame are

$$\left.\begin{aligned} e_a &= L\frac{di_a}{dt} + v_a \\ e_b &= L\frac{di_b}{dt} + v_b \\ e_c &= L\frac{di_c}{dt} + v_c \end{aligned}\right\} \tag{15}$$

where e_a, e_b, e_c are grid-side voltages, v_a, v_b, v_c are the inverter terminal voltages and L is the coupling inductance.

On converting the voltage (15) into synchronous d-q reference frame, we have

$$\left.\begin{aligned} e_d &= L\frac{di_d}{dt} - \omega L i_q + v_d \\ e_q &= L\frac{di_q}{dt} + \omega L i_d + v_q \end{aligned}\right\} \tag{16}$$

Usually, the load current and either of the grid or inverter currents are required to compensate the load reactive power

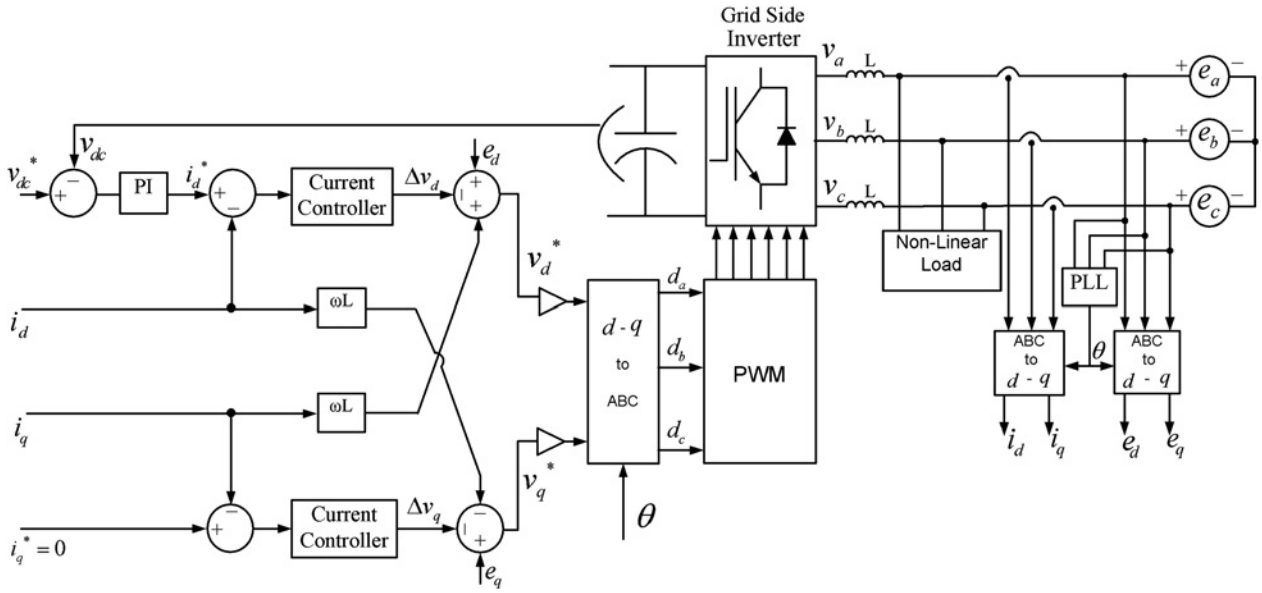

Figure 4 *Grid-side converter control*

and harmonics. This makes it necessary to have at least six current sensors in addition to four voltage sensors. In the proposed strategy, only three current sensors and four voltage sensors are used to force the grid current to be purely sinusoidal without having any knowledge of the inverter and load current profile. Now, the main aim of proposed controller is to generate the reference currents such that the grid always supplies only fundamental active power to the load at PCC. For UPF operation, the quadrature-axis reference current $i_q^* = 0$. The active power exchange between WECS and grid is directly proportional to the direct-axis current i_d and can be derived as

$$P = \frac{3}{2}(e_d i_d + e_q i_q) = \frac{3}{2} e_d i_d \tag{17}$$

This direct-axis current i_d is also responsible for regulating the dc-link voltage. Therefore the d-axis reference current i_d^* is generated from the PI controller for the dc-link voltage regulator expressed as

$$I_d^* = \left(K_{PV_{dc}} + \frac{K_{IV_{dc}}}{S}\right)(V_{dc}^* - V_{dc}) \tag{18}$$

where K_{PVdc} is proportional gain and K_{IVdc} is the integral gain of the dc-voltage regulator.

Generally, the standard PI controllers perform satisfactorily in forcing the grid current to track the reference current exactly. However, the presence of coupling terms in (16) deteriorates the performance of the PI regulator. To avoid this problem, the system can be decoupled in the form of a first-order linear dynamic system having better controllability, as follows

$$\left.\begin{aligned} 0 &= L\frac{\mathrm{d}i_d}{\mathrm{d}t} - \Delta v_d \\ 0 &= L\frac{\mathrm{d}i_q}{\mathrm{d}t} - \Delta v_q \end{aligned}\right\} \tag{19}$$

where, the output signals, Δv_d and Δv_q are derived from inner current controller loops as

$$\left.\begin{aligned} \Delta v_d &= K_p(i_d^* - i_d) + K_i \int (i_d^* - i_d)\,\mathrm{d}t \\ \Delta v_q &= K_p(i_q^* - i_q) + K_i \int (i_q^* - i_q)\,\mathrm{d}t \end{aligned}\right\} \tag{20}$$

Inclusion of these decoupled terms in (16), results in the reference d-q voltages of the inverter as follows

$$\left.\begin{aligned} v_d^* &= e_d + \omega L i_q - \Delta v_d \\ v_q^* &= e_q - \omega L i_d - \Delta v_q \end{aligned}\right\} \tag{21}$$

The reference d-q voltages obtained from (21) are transformed into a-b-c reference voltages with the help of grid voltage phase angle θ. The grid synchronising phase angle can be extracted using the phase lock loop technique. The reference voltages are then applied to the PWM controller to generate control signals for the grid-side inverter. The complete control diagram of the grid-side inverter is shown in Fig. 4.

4 Simulation results and discussion

The proposed control strategy for PMSG-based variable speed WECS is simulated using MATLAB/SPS under different operating conditions. The simulation results in Fig. 5 show the traces of wind speed, the generator

doi: 10.1049/iet-pel.2009.0132

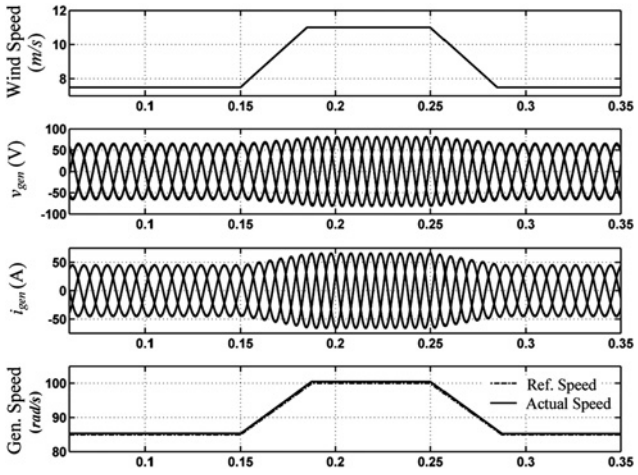

Figure 5 *Simulation results for MPPT*

terminal voltage (v_{gen}), generator terminal current (i_{gen}) and the generator rotor speed (ω_r). In Fig. 6, the simulation results for grid voltage (v_{grid}), grid current (i_{grid}), load current (i_{load}) inverter current (i_{inv}) and dc-link voltage (v_{dc}) are shown. In Fig. 7, the power flow between the inverter, grid and load is analysed under fluctuating wind and non-linear load conditions. Furthermore, an efficiency curve (η) obtained using wind generator power and the actual inverter output power is also shown in Fig. 7.

4.1 Performance of the generator-side controller

The simulation results for variable speed operation of the wind turbine are shown in Fig. 5. A variable input torque in proportion to wind speed is applied to PMSG and accordingly reference speed is calculated using the MPPT algorithm. Initially the applied wind speed is considered as 7.5 m/s. This makes the generator rotate at a speed of 85 rad/s. The corresponding generator voltage and current are found as 50 V and 45 A, respectively. At $t = 0.15$ s, the

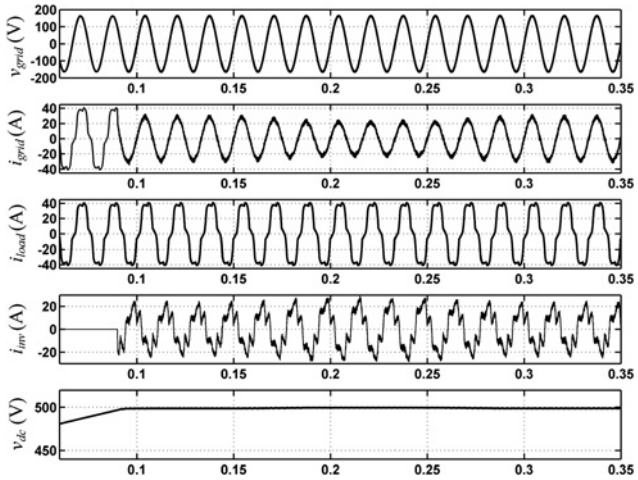

Figure 6 *Simulation results: performance of the proposed control approach*

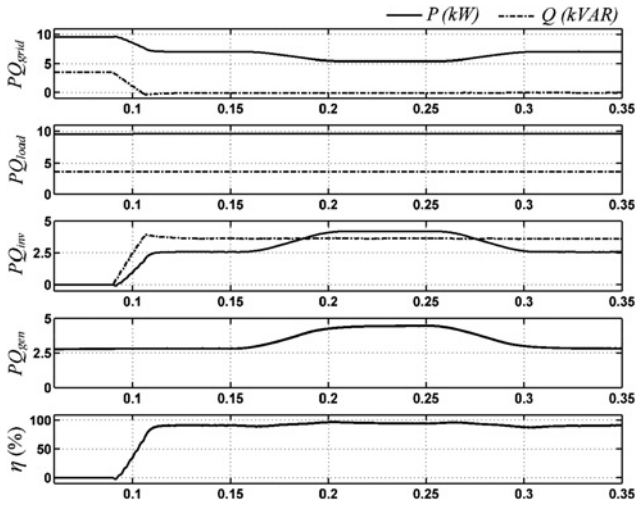

Figure 7 *Simulation results: power flow under different operating conditions*

wind speed starts increasing and reaches a new value of 11 m/s. In response to this, the generator speed also starts increasing and settles at a new value of 100 rad/s. The corresponding increase in generator voltage and current can also be noticed from Fig. 5. At time $t = 0.25$ s, the wind speed starts decreasing and reaches the same value as in the beginning. The respective change in generator speed, voltage and current can also be easily noticed. From the simulation results, it is evident that the generator follows the reference speed very closely. The effect of change in wind speed can also be verified from the amount of current and active power injected into the grid by the grid-side inverter as shown in Figs. 6 and 7, respectively.

4.2 Performance of the grid-side controller

The grid-side inverter is actively controlled to inject the generated active power as well as to compensate the harmonic and reactive power demanded by the non-linear load at PCC, such that the current drawn from grid is purely sinusoidal at UPF. The simulation results in Fig. 6 show the grid voltage, grid current, load current, inverter current and dc-link voltage. The load current consists of active, reactive and harmonic components. Initially, the grid-side inverter is intentionally switched off, just to demonstrate the capabilities of the proposed controller. Thus, the grid supplies the load current harmonics and reactive power demand, and therefore during this time period, the grid current profile is identical to the load current profile. At time $t = 0.09$ s, the grid-side inverter is switched on and the inverter starts injecting the current which is the sum of harmonic component, reactive component of non-linear load and active component in proportion to the generated wind power. Owing to this, the grid supplies the sinusoidal current at UPF and at a reduced magnitude depending on the amount of active power supplied by the inverter. At time $t = 0.15$ s, the

current injected from inverter increases due to increase in wind power, resulting in the proportional reduction in grid current. At $t = 0.25$ s, the injected inverter current starts decreasing with decrease in wind velocity and in response to this, the grid current starts increasing to meet the load demand. The dc-link voltage is maintained at a constant level of 500 V irrespective of any change in grid operating conditions.

Fig. 7 shows the simulation results for power flow under different wind turbine speeds. Initially, the grid-side inverter is not connected to the grid, and so the load active and reactive power demand of 9.6 kW and 4 kVAR is supplied by the grid. At time $t = 0.09$ s, the inverter is connected with the grid and it starts supplying the active as well as reactive power. Now the inverter feeds wind-generated active power of 2.4 kW and the grid supplies the remaining 7.2 kW to meet the load active power demand of 9.6 kW. Here it should be noted that the reactive power demand of 4 kVAR is completely supplied from the inverter in order to achieve UPF operation of the grid. At time $t = 0.15$ s, the injected active power of inverter starts increasing due to increase in wind speed and accordingly, the grid active power decreases. At this condition, the active power supplied from the inverter is 4.2 kW, and therefore 5.4 kW power is supplied from the grid to meet 9.6 kW active load demand. Again at time $t = 0.25$ s, the active power supplied from inverter starts decreasing with the decrease in wind velocity and corresponding change can be noticed in the grid active power.

In Fig. 7, the generator terminal power is also shown, which is slightly higher than the inverter-injected active power because of the losses in two back-to-back converters. These losses are found to be approximately 200 watts. The % efficiency (η) of the proposed system varies from 92 to 97%.

5 Experimental verification

A scaled hardware prototype is developed to validate the proposed control strategy. Two back-to-back connected converters with a common dc-link are used to realise the wind energy conversion system. One converter supplies the variable active power to the dc-link, whereas the other injects this active power as well as the reactive power and harmonics demanded by the loads at PCC. The control system is implemented using DS1104 DSP of dSPACE. The switching frequency of 5 kHz is used to control the IGBT-based voltage source converter.

To highlight the capability of the proposed control approach, the grid-side inverter operation is explained in two different modes of operations. The experimental results are given in Figs. 8–10. All the voltage and current waveforms are captured utilising an oscilloscope, whereas, the active and reactive powers are captured using ControlDesk Developer environment in real time. The load connected to PCC is considered as a non-linear load which

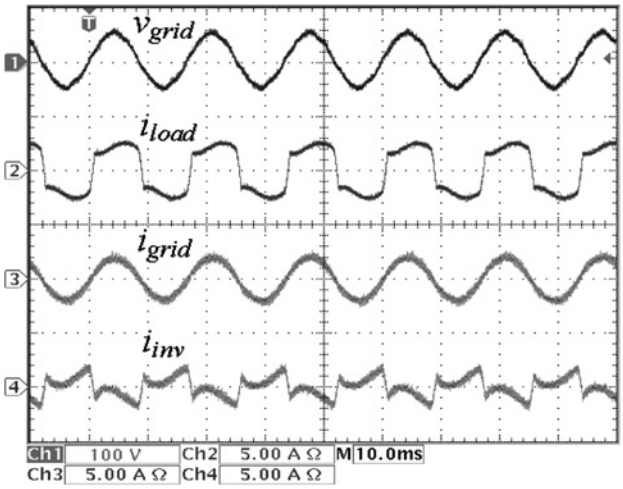

Figure 8 *Experimental results: performance of the proposed approach under partial load active power support and power quality enhancement*

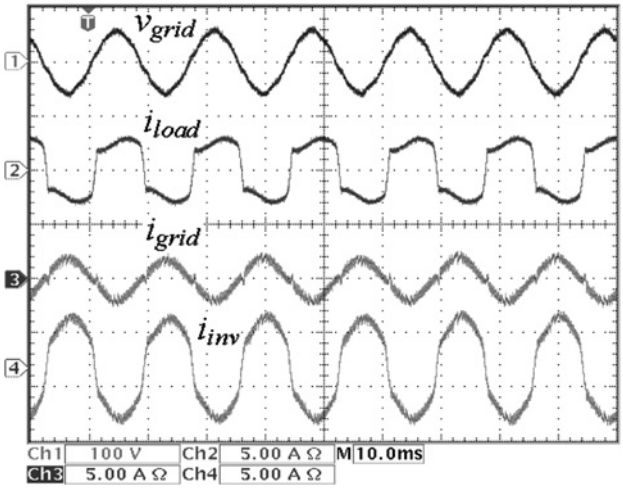

Figure 9 *Experimental results: performance of the proposed approach under active power support to the grid mode*

draws a distorted current [Fig. 8, trace-2] with total harmonics distortion (THD) of 28%.

5.1 Mode-I: partial load active power support

In this mode of operation it is considered that the WECS generates certain amount of power which is available at the dc-link. However, this available power from WECS is not enough to support the full load. The experimental results during this operating condition are shown in Fig. 8. The grid-side inverter adequately manages this power and supports the non-linear load in such a way that it maintains the sinusoidal grid current. The grid-side inverter injects the current which is the sum of harmonics component and generated active power component, can be noticed from

doi: 10.1049/iet-pel.2009.0132

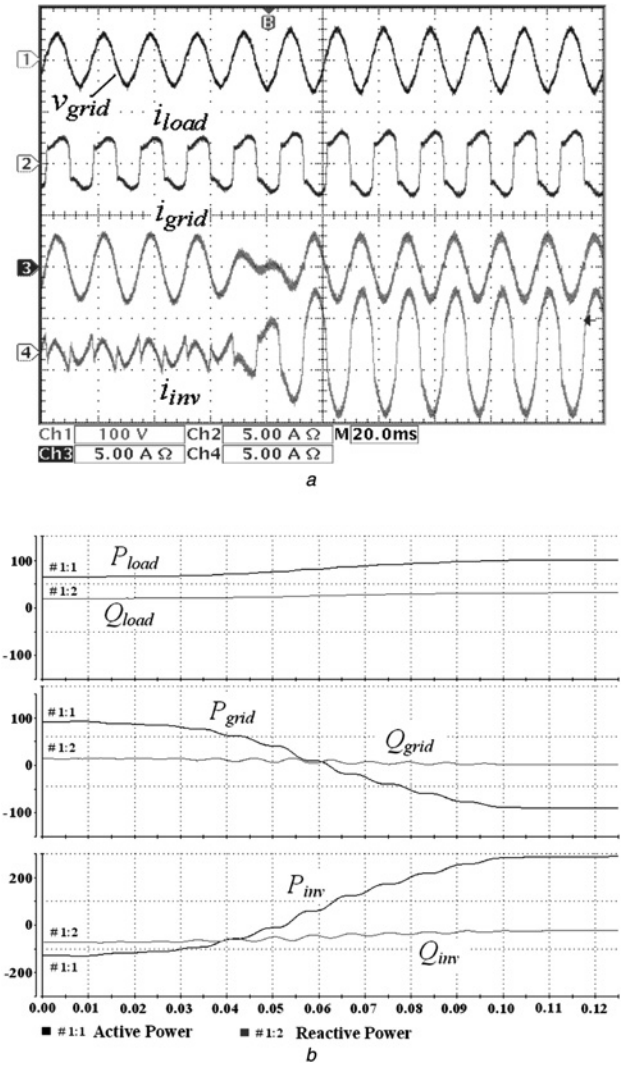

Figure 10 *Experimental results: dynamic performance of proposed approach*

Fig. 8, trace-4. The reduction in grid current magnitude [Fig. 8, trace-3] also justifies the aforementioned operation. The grid-side current THD is found to be 2.3%.

Here the UPF grid operation can also be noticed from Fig. 8 by comparing trace-1 and trace-3, which are in the same phase. This indicates that the grid supplies only fundamental active power to non-linear load (the reactive power supplied is almost zero), whereas the grid-side inverter supplies the generated active power and full load reactive power locally. The grid-side inverter consumes small amount of active power to overcome the losses associated with switching devices and to maintain the dc-link voltage at a constant level.

5.2 Mode-II: active power support to the grid

In this mode it is considered that the WECS generates power in excess to load power demand at PCC. The experimental results under this mode of operation are shown in Fig. 9. Since the power available at the grid-side inverter is more than the load power demand, the proposed controller manage this additional power effectively and feeds to the main grid. Under this condition the current injected by the grid-side inverter, as shown in Fig. 9 (trace-4), is the sum of load current and current supplied to the grid. The grid current profile is shown in Fig. 9 (trace-3). Here, the out-of-phase relationship between the grid voltage and current justifies the fact that the additional generated power is injected into the main grid effectively at UPF, whereas load reactive power demand is fully met by the grid inverter locally.

5.3 Dynamic performance of proposed control approach

Fig. 10 shows the experimental results to validate the dynamic performance of the proposed control approach under different modes of operation. Initially, it is considered that the system is working under mode-I operating condition (i.e. non-linear load current harmonics and reactive power compensation). The power at dc-link is suddenly increased that can be noticed from Fig. 10*b*. The proposed controller manages this additional power precisely and feeds to the main grid. A smooth changeover from mode-I operating condition to the mode-II can be noticed. The corresponding changes in active and reactive powers of the voltage source inverter and the main grid can be viewed from Fig. 10*b*.

6 Conclusion

The performance of PMSG-based variable speed WECS has been demonstrated under varying wind conditions. The proposed controller incorporates the grid synchronisation of the distributed generating system. The grid-side inverter is able to inject the generated power into the grid with harmonic and reactive power compensation of non-linear load at PCC, simultaneously. The system works satisfactorily under dynamic conditions. The simulation results supported by experimental results validate the effectiveness and robustness of the proposed controller under different operating modes. The experimental results under a non-linear load with current THD of 28% confirm that the grid-side inverter can effectively inject the generated active power along with the load current harmonics and reactive power and thus, it maintains a sinusoidal and UPF current at the grid side with THD of 2.3%.

7 Acknowledgments

The authors would like to thanks the Ministry of Social Justice and Empowerment, Govt. of India for the scholarship and the High Commission of India, Ottawa, Canada for the timely financial support to carry out this research work.

8 References

[1] 'Grid code for high and extra voltage', E.ON Netz GmbH, Bayreuth, Germany, August 2003. Internet, http://www.eon-netz.com/Ressources/downloads/enenarhseng1.pdf

[2] 'Connection of wind turbines at the grid under 100 kV'. Technical regulations T.F. 3.2.6, Eltra/Elkraft, July 2004. Internet, http://www.eltra.dk

[3] 'IEEE standard for interconnecting distributed resources with electric power systems', IEEE15471, 2005

[4] SENJYU T., KINJO T., FUJITA H., AICHI: 'Analysis of terminal voltage and output power control of wind turbine generator by series and parallel compensation using SMES'. IEEE 35th Ann. Power Electronics Specialists Conf., June 2004, vol. 6, pp. 4278–4284

[5] MORREN J., DE HANN S.W.: 'Ride-through of wind turbines with doubly-fed induction generator during a voltage dip', *IEEE Trans. Energy Convers.*, 2005, **20**, (2), pp. 435–441

[6] SACCOMANDO G., SVENSSON J., SANNINO A.: 'Improving voltage disturbance rejection for variable-speed wind turbines', *IEEE Trans. Energy Convers.*, 2002, **17**, (3), pp. 422–428

[7] MILLIGAN M.: 'Measuring wind plant capacity value' (National Renewable Energy Laboratory, Golden Colorado, USA)

[8] BOCCARD N.: 'Capacity factor of wind power realized values vs. estimates', *Elsevier Trans. Energy Policy*, 2009, **37**, pp. 2679–2688

[9] 'Capacity factors at Kansas wind farms compared with total state electrical demand', July 2007 to June 2008, http://www.kcc.state.ks.us/energy/charts/Wind Capacity Factors at Kansas Wind Farms Compared with Total State Electrical Demand.pdf

[10] MULJADI E., BUTTERFIELD C.P.: 'Pitch-controlled variable-speed wind turbine generation', *IEEE Trans. Ind. Appl.*, 2001, **37**, (1), pp. 240–246

[11] HEIER S.: 'Grid integration of wind energy conversion systems' (Wiley, Chicester, UK, 1998)

[12] JOHNSON G.: 'Wind energy systems' (Prentice-Hall, Englewood Cliffs, NJ, 1990)

[13] WESTLAKE A.J.G., BUMBY J.R., SPOONER E.: 'Damping the power-angle oscillations of a permanent magnet synchronous generator with particular reference to wind turbine applications', *IEE Proc. Electr. Power Appl.*, 1996, **143**, (3)

[14] KRAUSE P.C., WASYNCZUK O., SUDHOFF S.D.: 'Analysis of electric machinery' (IEEE Press, 1994)

[15] CARRASCO J.M., FRANQUELO L.G., BIALASIEWICZ J.T., *ET AL.*: 'Power-electronic systems for the grid integration of renewable energy sources: a survey', *IEEE Trans. Ind. Electron.*, 2006, **53**, (4), pp. 1002–1016

[16] ENSLIN J.H.R., HESKES P.J.M.: 'Harmonic interaction between a large number of distributed power inverters and the distribution network', *IEEE Trans. Power Electron.*, 2004, **19**, (6), pp. 1586–1593

[17] SLOOTWEG J.G., DE HAAN S.W.H., POLINDER H., KLING W.L.: 'General model for representing variable speed wind turbines in power system dynamics simulations', *IEEE Trans. Power Syst.*, 2003, **18**, (1), pp. 144–151

[18] LEONHARD W.: 'Control of electric drives' (Springer, New York, 1997)

[19] ASIMINOAEI L., BLAABJERG F., HANSEN S.: 'Harmonic detection methods for active power filter applications', *IEEE Ind. Appl. Mag.*, 2007, pp. 22–33

9 Appendix

The parameter used for PMSG Simulink model: three-phase, 12 kW, number of pole pair = 4, d-axis inductance $L_d = 0.001$ H, q-axis inductance $L_q = 0.001$ H, stator resistance $R_s = 3.85\ \Omega$, inertia $J = 2.5\,e^{-3}$ kgm^2, damping coefficient $B = 1.86e^{-3}$ Nm/rad/s and magnetic flux $\Psi = 0.118$ Wb.

The parameter used for experimental study: ac supply voltage = 35 V (rms), fundamental frequency = 60 Hz, reference dc-link voltage = 75 V, dc bus capacitor = 1200 μF/200 V, grid-side converter coupling inductance = 3 mH, non-linear load: diode bridge rectifier followed by R-L load with $R = 40\ \Omega$/5 mH, DSP sampling time = 45 μs and converter switching frequency = 5 kHz.

doi: 10.1049/iet-pel.2009.0132